ASME Early Career Technical Journal
2010 ASME Early Career Technical Conference, ASME ECTC
October 1-2, 2010, Atlanta, Georgia, USA

Method to Accurately Estimate Tesla Turbine Stall Torque For Dynamometer or Generator Load Selection

Tamir A. Emran, Ryan C. Alexander, Chris T. Stallings,
Mark A. DeMay, Matthew J. Traum*
Department of Mechanical & Energy Engineering
University of North Texas
Denton, Texas, USA

ABSTRACT

For experimental Tesla turbine measurements and characterization, conventional dynamometer diagnostics meant for small IC engines are challenging because Tesla turbines produce power at high angular velocity and low torque. Moreover, similar challenges arise when sizing generators for Tesla-turbine-based power generation. Often the minimum cut-in torque of a conventional dynamometer or generator exceeds the stall torque of the Tesla turbine at a desired set-point. To facilitate proper sizing of dynamometers/generators for Tesla turbine diagnostics and power generation, a simple, inexpensive, and accurate method is introduced to experimentally assess a Tesla turbine's static torque under a prescribed series of inlet conditions using a simple spring force gauge. This static torque measurement technique is validated by using it to select an appropriate brushed DC motor at the heart of a customized dynamometer to be used in future research. The Tesla turbine used in this current study successfully spun up the motor as anticipated.

Additionally an analytical technique is introduced, applicable to Tesla turbine configurations with four equally spaced inlet ports, to estimate the static torque produced by the turbine based on its measured un-loaded rotational velocity. This technique imagines a single turbine disk broken into four sections. Torque transmitted to the power shaft by shear force on each section when the disks are not spinning is estimated using laminar free stream flow over a flat plate. Despite its considerable inherent engineering assumptions, this model provides a reasonable orientation calculation for motor/generator sizing for service when coupled to a Tesla turbine. This model is validated by comparison to the above described experimental stall torque measurements. Good agreement is found, especially in the regime of highest turbine inlet flow velocity where a Tesla turbine would be expected to operate for power generation applications.

INTRODUCTION

Tesla turbines are bladeless rotating turbo-machinery components that transform enthalpy in a working fluid into shaft work. While their purpose is identical to conventional gas turbines, the mechanism of energy conversion in Tesla turbines is very different. Conventional gas turbines expand the working fluid over aerodynamic blades, producing a lift force on each blade that induces torque about a rotating drive shaft. Tesla turbines rely on fluid shearing force at the interface between the working fluid and an internal set of bladeless disks to generate torque about the drive shaft.

These two working fluid enthalpy extraction methods manifest power output, P, very differently; P is the product of torque, τ, and angular velocity, ω.

$$P = \tau\omega \tag{1}$$

Even if a conventional gas turbine and Tesla turbine were generating the same power output, the way this output would be measured and utilized is different. Conventional bladed gas turbines produce relatively high torque and low angular velocity compared to Tesla turbines, which typically produce low toque at high angular velocity.

Available modern diagnostic instruments for small rotating engines below 35 kW, the power output where many research Tesla turbines operate, include only dynamometers designed to measure high-torque, low-angular-velocity internal combustion (IC) engines. [1,2] These small commercial dynamometers, meant for IC engines, are not competent for Tesla turbine testing as the dynamometer cut-in torque exceeds the Tesla turbine stall torque. ***Cut-in*** refers to the torque required to begin turning the dynamometer, while ***stall*** refers to a load torque slightly higher than what the turbine can generate at a particular set-point, which causes its rotation to slow below a desirable level or even stop. Moreover, commercial dynamometers for small IC engines cannot withstand the high angular velocities Tesla turbines produce. Coupling conventional dynamometers to Tesla turbines often requires a mechanical advantage system (i.e., pulleys or gears), which introduce their own friction losses that must be quantified separately. As a result, most Tesla turbine research begins with development of a custom-built high-speed, low torque dynamometer. [3,4]

One relatively inexpensive approach to custom Tesla turbine dynamometer design is to drive the shaft of a commercial-off-the-shelf electric motor. This approach enables measurement of turbine torque output by either 1) measuring of the shaft torque directly at the shaft coupling or 2) measuring the force required to prevent the motor housing from rotating. Different motor loads are set to extract a turbine power curve as a function of torque or angular velocity. An optical or Hall Effect sensor measuring angular velocity of the shaft provides

*Corresponding author:
mtraum@unt.edu, (940) 565-3446

the remaining needed information to solve Eq. 1 for P. As a corollary, to generate electrical power from a Tesla turbine, a high-speed electric generator could be coupled to the power shaft.

One difficulty in coupling an electric motor or generator to a Tesla turbine for diagnostic or power generation applications is that the electric motor/generator cut-in torque might exceed the Tesla turbine's stall torque. The same problem arises when trying to mate a conventional IC engine dynamometer to a Tesla turbine. To specify an appropriate motor/generator for diagnostics or power generation, an inexpensive and straightforward Tesla turbine stall torque calculation method is needed to ensure turbine stall torque exceeds motor/generator cut-in speed at desired set-point conditions. Moreover, to facilitate informed engineering design of both Tesla turbines and their associated dynamometers (or generators), development of a predictive analytical technique for stall torque estimation is warranted.

In this paper, a simple, accurate, and inexpensive technique for measurement of Tesla turbine stall torque is reported, which we follow with an analytical method that predicts stall torque as a function of desired turbine set-point parameters. The quantitative results arising from these techniques are compared to each other to provide validation and then used to select an appropriate brushless DC motor for a custom dynamometer that is slated for future Tesla turbine testing.

BACKGROUND

Despite the extensive body of literature on Tesla turbine modeling, design, and testing (an excellent recent review is given by Rice [5]) no literature could be found reporting Tesla turbine stall torque measurement or predictive analysis techniques.

The initial Tesla turbine invention and patent disclosure [6] has generated prolific academic research on bladeless turbine design, diagnostics, and optimization. After Tesla's patent expired, Leaman [7] experimented using a four-disk Tesla turbine with a novel hollow power shaft allowing for fluid exhaust. He evaluated different disk surface finishes, bearing designs, and nozzle configurations to maximize efficiency resulting in a parabolic relationship between angular velocity and efficiency with a peak efficiency of 8.6% at 85.75 watts (0.115 hp). This early work laid the foundation for over 60 years of subsequent research.

Beans [8] analyzed the similarities between Tesla turbines and drag turbines. He noted that because no lift is generated in either configuration, both these turbine types rotate no faster than the onset fluid velocity; a key phenomenon applied to the stall torque analysis presented in this current paper. Murata et al [9] analyzed whether flow between Tesla turbine disks is laminar or turbulent and found that the flow is laminar within the turbine except on the inner and outer disk peripheries where instead they observed vortex flow. Based on this analysis, the analytical models used in this paper assume laminar flow between the disks. Recent improvements in computer modeling capability enable visualization and analysis of flow inside the Tesla turbine housing. For example, Harwood [10] simulated internal Tesla turbine flows in ANSYS to corroborate the observed results of Murata et al [9] by demonstrating existence of internal Tesla turbine vortex rotational flow structures and back pressure. Harwood [10] also found that peak Tesla turbine efficiency is achieved at low Reynolds number, which further validates the assumption of laminar flow used in our analysis as a desirable Tesla turbine operating condition.

Guidance for the dynamometer experimental apparatus described in the "Conclusions" section of this current paper was gleaned from Hoya and Guha [3] who comprehensively described how to design and build a Tesla turbine and diagnostic Tesla turbine dynamometer. Finally, no review of the Tesla turbine literature would be complete without acknowledging the prolific and on-going contributions of Swithenbank [11] to this field.

EXPERIMENTAL METHODS AND TECHNIQUES

An Obi Laser SSTG-001 Tesla turbine [12] was used in the experiments here described. This turbine is made of stainless steel and contains four disks of 37.6 mm outer radius (R_{outer}) and 34.0 mm inner radius (R_{inner}) each spaced apart by 5.0 mm. The turbine has four air inlets evenly spaced around the periphery, and it has four outlet ports near the center. The power shaft radius is 4.0 mm. The specific disk and nozzle shapes are proprietary and cannot be disclosed, but (as will be explained below) these detailed geometric features do not impact the general experimental or analytical results.

Shop air at constant pressure was introduced to the experimental apparatus through a regulator-filter combination that kept the supply line pressurized between 90 and 120 psi regardless of the flow demand from the turbine. A smaller control regulator connected to the turbine inlet manifold provided precise turbine inlet pressure adjustment; during the experiment, the control regulator was adjusted from 15 psi to 85 psi in 5 psi increments to establish the range of experimental set-points. The pressure regulator set-point uncertainty was ±2.5 psi. 85 psi was never exceeded to ensure fluctuations in the supply line pressure (90 – 120 psi) did not adversely impact results. The inlet manifold split the flow from the regulator into four paths and delivered the working fluid to each of the turbine inlets as shown in Figure 1.

Experimental stall torque measurements proceeded in two stages. First, the turbine was set up to spin with no load on the shaft. Output shaft angular velocity for the turbine was determined using a Neiko 20713A digital laser photo tachometer that registered the rotational frequency of a piece of black electrical tape fixed to the shaft. For each pressure set point from 15 to 85 psi, 20 unique rotational frequency data points were taken, and rotational velocity was calculated from shaft geometry. The average of these 20 readings was the reported angular velocity while the standard deviation among them was the reported measurement uncertainty.

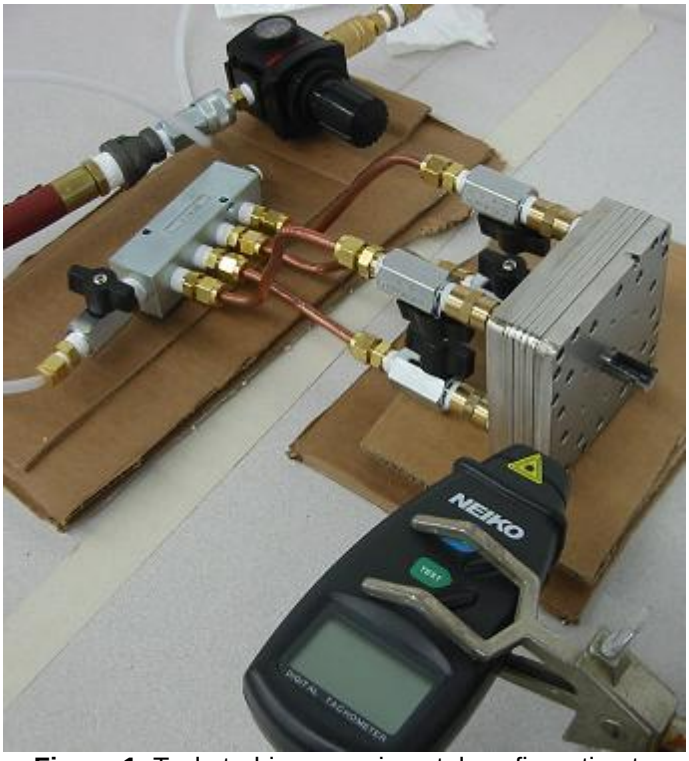

Figure 1: Tesla turbine experimental configuration to measure un-loaded rotor rotational velocity. The manifold splitting the flow into four turbine inlets appears to the left of the image. The cardboard upon which the components are sitting reduced vibration during normal operation.

At first glance, it may seem odd to measure a turbine's stall torque by allowing it to run unloaded: the antithesis of the stall condition. However, as there was no direct means to measure the internal turbine flow velocity from the inlet nozzles, unloaded turbine disk linear velocity at R_{outer} approximated the fluid flow velocity. As mentioned above, Beans [8] argued that the linear velocity of the outer edge of a Tesla turbine disk cannot exceed internal air flow velocity because momentum transfer from the flow to the disk occurs entirely by shear. In fact, in the limit where there is no outside friction force (i.e., no bearing friction) to slow the rotating disks of an unloaded Tesla turbine, the linear velocity of the disk assembly's outer edge will ***exactly match*** the flow velocity from the nozzles.

We validated our assumption that dissipative friction forces slowing our Tesla turbine's rotation are extremely small by quantitative calculation and qualitative experiment. The frictional torque, $\tau_{bearing}$, for a shaft bearing supporting a force, F, on that shaft is

$$\tau_{bearing} = \mu F R_{shaft} \qquad (2)$$

where μ is the coefficient of friction for the Tesla turbine bearings (μ = 0.0015). Using Eq. 2, the largest bearing friction torque encountered during any static test reported in this current paper was 4.03 x 10^{-5} N-m. To put this value in perspective, the smallest stall torque encountered during any static test reported herein was 1.03 x 10^{-3} N-m; 25.6 times larger. Moreover, in the unloaded tests where disk velocity was measured to approximate nozzle velocity, there was no linear force through the shaft supported by the bearing. So, the given 4.03 x 10^{-5} N-m friction torque estimate is an upper bound on the actual friction torque present during these measurements. To qualitatively demonstrate that the magnitude of rotational friction torque is miniscule, the unloaded turbine was spun up to steady state at 85 psi inlet pressure and allowed to spin down due to friction. This process took over 15 minutes to stop the turbine. These two friction quantification approaches demonstrate that friction forces are negligible when using the unloaded turbine rate of rotation as a surrogate to estimate internal flow velocity.

This internal flow velocity estimation approach is generally applicable to all Tesla turbines regardless of the specific blade configuration or nozzle geometry. As stated above, specific internal geometry does not affect the desired outcome, which is an estimation of the fluid velocity over the Tesla turbine disks when they are fixed and stationary. The resulting inferred flow velocity as a function of inlet pressure is applied to the analytical stall torque estimation method outlined in the "Stall Torque Calculation Method" section below.

In the second measurement stage, the static torque produced by the turbine was directly measured across the same range of inlet pressures used to determine internal flow velocity, 15 – 85 psi. Importantly, the static torque and stall torque definitions used in this paper are subtly different. ***Static torque*** is measured through a force gauge that intentionally holds the Tesla turbine power shaft stationary so it cannot spin. ***Stall torque*** is encountered while the turbine is spinning, and the demanded load increases above the available turbine torque at its particular set-point conditions and angular velocity. While gas from the internal turbine nozzles continues issuing at a set velocity, the turbine slows (e.g., stalls) in response to the higher load to a lower rotational velocity. At this new slower rotation rate, the difference between the internal fluid flow velocity and rotating disk velocity is higher and the resulting produced torque is greater. Thus, a turbine can stall without stopping. However, static torque is a special subset of stall torque in which the demanded load is just great enough to cause the turbine to stop spinning altogether. In this condition, the velocity difference between the internal flow velocity and blade velocity is maximized, and therefore the resulting torque produced by the turbine is maximized for the given set-point conditions. Measured static torque is thus an upper bound on the turbine's stall torque at a particular set-point condition.

Turbine static torque was measured using a spring force gauge. One end of the spring force gauge was anchored to a protruding drawer handle. Then approximately 20 cm of fishing line connected the other end of the spring force gauge to the turbine power shaft. The spring gauge was carefully positioned to ensure its force measurement remained tangent to the shaft. A burst of air into the turbine allowed the fishing line to wind around the shaft until it was tight and its tension stalled the

turbine into a static condition. See Figure 2 for details of this set-up. Only one layer of fishing line winding was allowed to accumulate on the shaft to maintain precise control over the shaft lever arm (i.e., the power shaft radius). Static force generated by the turbine, F, was measured at turbine inlet pressures from 15 to 85 psi at 5 psi increments, and associated stall torque, τ_{stall} at each set point was calculated:

$$\tau_{stall} = R_{shaft} F \tag{3}$$

Figure 2: Simple Tesla turbine static torque measurement configuration showing spring gauge alignment.

STALL TORQUE ANALYTICAL CALCULATION

Our analytical Tesla turbine stall torque approximation relies upon the exact equation for shear induced by laminar flow over a flat plate.

$$\tau_w = 0.332 U^{3/2} \sqrt{\frac{\rho \mu}{x}} \tag{4}$$

where τ_w is the shear stress along the wall of a turbine disk, U is the linear velocity of flow along the turbine disk, ρ and μ are the working fluid density and viscosity respectively, and x is a coordinate location along a flat disk from a turbine inlet nozzle.

Importantly, the linear disk velocity measured during the unloaded turbine tests described above approximates U in Eq. 4. As illustrated graphically in Figure 3, the analytical model is developed by breaking a complete turbine disk into four separate pieces (one-quarter disk for each inlet port). Each piece has a length equal to a quarter of the disk's circumference, and each has a width equal to the difference between the outer and inner disk radii. The shear force induced by the flow over these four separate pieces is imagined to act at a single point at the center of each plate. The resulting torque is calculated by multiplying these forces by a lever arm equal to the distance from the disk center to half the disk's width (R_{ave} in Figure 3),

$$R_{ave} = \frac{R_{outter} + R_{inner}}{2} \tag{5}$$

The torque then arising from one exposed face of the four flat plates representing a single turbine disk is

$$T = 4F\ R_{ave} \tag{6}$$

where the net force on each plate, F, is the product of shear force and surface area. In differential form this expression is

$$dF = \tau_w\, dA \tag{7}$$

where a differential element of this flat plate, *d*A, is defined as

$$dA = (R_{outter} - R_{inner})dx \tag{8}$$

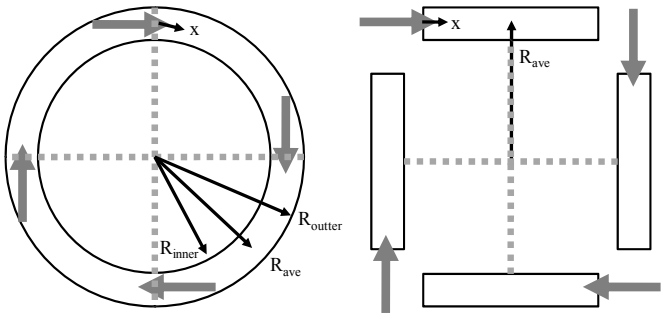

Tesla Turbine Disk **Approximate Flat Plate Model**

Figure 3: The analytical static torque model simplifies the geometry of a Tesla turbine disk (left) by imagining it separated into four flat plates. Force on these four plates is estimated using the laminar flat plate shear equation. The product of shear force and the lever arm, R_{ave}, calculates the resulting static torque.

Once the torque on one disk face is estimated, the result is multiplied by 8 (the total number of disk surfaces) to provide the overall estimate of the Tesla turbine static torque, which (as explained above) is an upper bound on the expected stall torque for given set-point conditions.

Combining Equations 4, 7, and 8 and integrating from $0 \leq x \leq \pi/2\ R_{ave}$ (the length of one plate is a quarter of the disk's circumference) gives

$$F = \left[0.332U^{3/2}\sqrt{\rho\mu}\right](R_{outter} - R_{inner}) \int_0^{\frac{\pi}{2}R_{ave}} \sqrt{\frac{1}{x}}\,dx \qquad (9)$$

Substituting the expression in Eq. 9 into Eq. 6, completing the integration, and multiplying by 8, the total number of disk faces engaged in shear momentum transfer gives the desired equation:

$$T = 32\left(0.664U^{3/2}(R_{outter} - R_{inner})R_{ave}\sqrt{\rho\mu\frac{\pi}{2}R_{ave}}\right) \qquad (10)$$

We will certainly concede that this model is a very rough approximation to the true Tesla turbine geometry and internal flow structure. Moreover, this model necessitates many additional engineering assumptions: 1) flow over the disks is laminar, 2) the velocity profile between the disks approximates flow over a flat plate instead of plane poiseuille flow, 3) the radial spiraling component of the flow adds negligible contribution, and 4) all of the disks are fully engaged by flow at free stream velocity U. Nonetheless, the reasonable correspondence between measured static torque values of the Tesla turbine and this simple analytical model is compelling enough to make it a valuable orientation calculation for estimation of Tesla turbine stall torque.

RESULTS AND DISCUSSION

A comparison between experimentally measured Tesla turbine stall torque and the analytical stall torque model of Eq. 10 is illustrated in Figure 4. While turbine inlet pressure is the adjustable parameter for both data sets, it has limited physical meaning as an abscissa. Thus, the inlet pressure was used as a parametric variable linking stall torque to inlet flow velocity to provide a more physically meaningful and relevant plot.

Two curves representing the analytical solution of Eq. 10 are plotted. While Eq. 10 represents a model solution, experiential measurement is required to determine U. Therefore upper bound and lower bound curves are plotted based on experimental uncertainties associated with measuring the Tesla turbine inlet pressure, the rate of power shaft rotation, and the outer radius of the Tesla turbine disk assembly.

As shown in Figure 4, the model of Eq. 10 tends to over-predict the measured Tesla turbine static torque for inlet velocity, V, up to 100 m/s, and it under-predicts measured values for V > 100 m/s owing to a jump in measured static torque at this speed. We attribute this jump near 100 m/s to a change in the fluid flow regime around this velocity. One possibility is changeover from laminar transition flow to turbulent flow in the gaps between the disks at this velocity. The internal flow Reynolds number (using disk spacing as the characteristic dimension) is about 3200 at flow V = 100 m/s, which is toward the top end of the transition flow regime, with fully turbulent flow (Re > 4000) occurring at about V = 125 m/s. Another flow regime change that may occur around inlet V = 100 m/s is onset of compressibility effects as the Mach Number is about 0.3. We would, however, expect these compressible flow effects to appear gradually instead of appearing instantaneously as was experimentally observed.

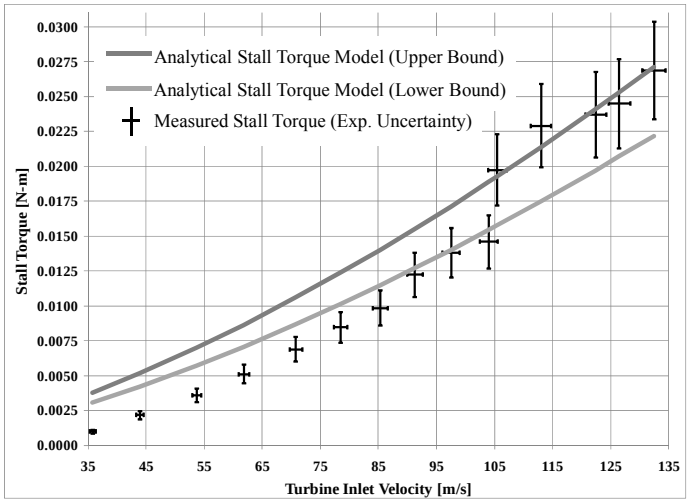

Figure 4: A comparison between the bounding values of the simple analytical model and the measured stall torque data reveals reasonable agreement given the liberal assumptions inherent in the model. This approach provides a good orientation calculation to guide sizing of motors/generators attached to a Tesla turbine.

Another important point is that Eq. 10 was derived for a Tesla turbine with four equally spaced gas inlet ports distributed about the periphery of the turbine housing. As a result, the disk was modeled by imagining it split into four sections where each section would see a refreshed free stream flow owing to the presence of its local inlet. Other Tesla turbines have different inlet numbers and configurations, which may be less amenable to the modeling approach used here. For example, flow inside a Tesla turbine with a single port would have to traverse the entire circumference of the disk before being refreshed. This flow type could transition to turbulence sooner or form a significantly different velocity profile far from the inlet port that what occurs for the N = 4 configuration. As a first step to modeling stall torque in Tesla turbines with N inlet ports when $N \neq 4$, we suggest re-deriving Eq. 10 by splitting the turbine disk into N sections.

To address the model's validity for Tesla turbine configurations where $N \neq 4$, we have plumbed our Obi Laser SSTG-001 Tesla turbine with on/off valves at the four inlet ports (see Figure 1), and in the future we plan to run tests with

N = 3, 2, and 1 port(s) active and to extend the predictive analytical model in this paper to additional inlet configurations.

CONCLUSIONS

Using conventional dynamometer diagnostics meant for small IC engines (35 kW or less) is impractical to characterize Tesla turbines as these blade-less turbines produce power at high angular velocity and low torque. Often the cut-in torque of the dynamometer exceeds the stall torque of the Tesla turbine, motivating creation of customized dynamometers for Tesla turbine research.

To facilitate proper sizing of motor/generators for custom Tesla turbine dynamometers or power generation applications, we introduced a simple, inexpensive, and accurate method (which was demonstrated using our Obi Laser SSTG-001 Tesla turbine) to experimentally assess the turbine's static torque under a prescribed series of inlet conditions. Noting that static torque is the upper bound of stall torque for a particular turbine set-point condition, this method enabled quantitative and accurate sizing of turbine-coupled motor/generators. Measured stagnation torque was found to jump up noticeably around V = 100 m/s inlet velocity, a phenomenon we attribute to an abrupt change in the Tesla turbine internal flow structure under these conditions; possibly a change from laminar transitional flow to turbulent flow.

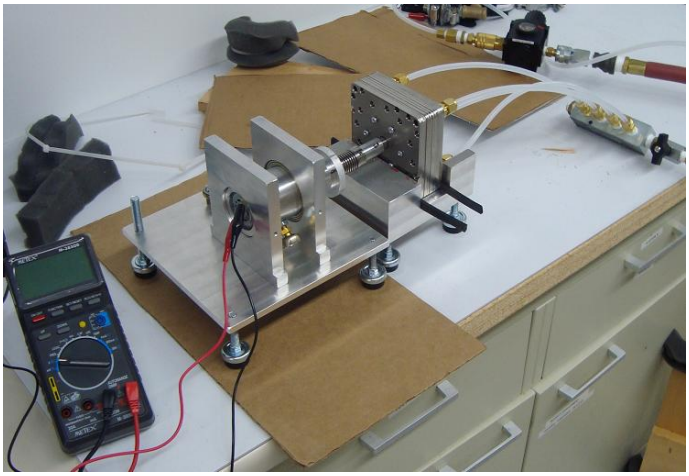

Figure 5: This custom Tesla turbine dynamometer was built around a particular brushed DC motor, which was specified to ensure it could be spun up by the available Tesla turbine based on tests using the static torque measurement technique described in this current paper.

In addition, we introduced an analytical technique, applicable to Tesla turbine configurations with four equally-spaced inlet ports, to estimate the static torque produced by the turbine based on its measured unloaded rotational velocity. This technique breaks a single turbine disk into four sections and solves for the torque induced on the power shaft by each section assuming the shear stress follows the exact solution for laminar free stream flow over a flat plate. Despite the significant engineering assumptions and geometric simplifications inherent in this model, it provides a good orientation calculation for motor/generator sizing, particularly in the high inlet velocity flow regime where a Tesla turbine is likely to operate for power generation.

While using the static torque measurement technique outlined in this current paper, we designed and build a dynamometer for Tesla turbine performance testing, shown in Figure 5. At the dynamometer's heart is a Banebots RS-550 brushed DC motor [13] rated to 19,300 rpm. We have already successfully spun up this motor with the Obi Laser SSTG-001 Tesla turbine, further validating our experimental static torque measurement technique.

ACKNOWLEDGEMENTS

This research was funded by the National Science Foundation Research Experiences for Undergraduates (RUE) program (NSF Grant Number EEC-100485) and by the Center for the Study of Interdisciplinarity at the University of North Texas (UNT) <http://www.csid.unt.edu/>. Additional UNT support was provided through the Junior Faculty Summer Research Fellowship and the Research Initiation Grant Program. The authors gratefully acknowledge Solar Logic, Inc. of Muenster, TX, which provided a Tesla-turbine-focused summer co-op experience for the lead author that provided, in part, motivation for this research. All undergraduate students working on this project are members of the UNT Texas Undergraduate Researcher Incubator (TURI), an organization which fast-tracks undergraduates into meaningful early research experiences.

REFERENCES

[1] Trik-Dyno, LLC Web site (2010), URL: http://www.trik-dyno.com/ , accessed 9/6/2010.

[2] Land-and-Sea, Inc. Web site (2010), Dyno-mite Dynamometer, URL: http://www.land-and-sea.com/ , accessed 9/6/2010.

[3] Hoya, G. P. and Guha, A. (2009) "The Design of a Test Rig and Study of the Performance and Efficiency of a Tesla Disk Turbine." *ASME Journal of Power and Energy*, Vol. 223, pp. 451-665.

[4] Kusumba, S. (2004) "Dynamometer Proportional Load Control," Master's Thesis, Cleveland State University, URL: http://academic.csuohio.edu/embedded/Publications/Thesis/Srujan_thesis.pdf , accessed 9/6/2010.

[5] Rice, W. (2003) "Tesla Turbomachinery." Chapter in, Handbook of Turbomachinery, 2nd Ed: Revised and Expanded, eds. E Logan, Jr and R. Roy, pp. 867-880.

[6] Tesla, N. (1913), "Turbine," United States Patent 1,061,206. 6 May, 1913.

[7] Leaman, A.B. (1950) “The Design, Construction and Investigation of a Tesla Turbine,” Master’s Thesis, University of Maryland.

[8] Beans, E. W. (1961) “Performance Characteristics of a Friction Disk Turbine,” Doctoral Dissertation, Pennsylvania State University.

[9] Murata, S., Yukata, M., and Yoshiyuki, I. (1976) “A Study on a Disk Friction Pump,” *Bulletin of the Japanese Soceity of Mechanical Engineer*s, Vol. 19, pp. 168-178.

[10] Harwood, P. (2008) “Further Investigation into Tesla Turbomachinery,” Senior Project Report, Mechanical Engineering Department, University of Newcastle, URL: http://www.scribd.com/doc/27375893/tesla-pumps-and-compressors , accessed 9/6/2010.

[11] Swithenbank, A. M. (2008) Web site: “The Tesla Boundary Layer Turbine”,
URL: http://www.stanford.edu/~hydrobay/lookat/tt.html , accessed 9/6/2010.

[12] Obi Laser Products Web site (2010), URL: http://www.obilaser.com/ , accessed 9/6/2010.

[13] Banebots Robot Parts Web site, (2010) “Banebots RS-550 brushed DC motor,” URL: http://banebots.com/pc/MOTOR-BRUSH/M2-RS550-120 , accessed 9/6/2010.